

In Situ STM Study of Electrocrystallization of Ag on Ag(111)

Silvana G. García^{*,a}, Carlos E. Mayer^{a,#}, Daniel R. Salinas^a and Georgi Staikov^b

^a Instituto de Ingeniería Electroquímica y Corrosión (INIEC), Dpto. de Ing. Química, Universidad Nacional del Sur, 8000 Bahía Blanca, Argentina

^b Institut für Schichten und Grenzflächen, ISG 3, Forschungszentrum Jülich, D-52425 Jülich, Germany

O processo de eletrocristalização foi estudado para o sistema Ag(111)/Ag⁺, SO₄⁻ utilizando Microscopia Eletrônica de Tunelamento (STM) *in situ*. Os resultados mostram que a deposição de Ag ocorre preferencialmente nos cantos dos degraus seguidos de um mecanismo de crescimento camada a camada, mas a polarização e as condições de imagem afetam grandemente a cinética local desse processo. Para potenciais da sonda do STM mais positivos do que o potencial de equilíbrio Ag/Ag⁺, uma dissolução local do substrato, sob a sonda é observada mesmo em sobrepotenciais de substrato muito negativos, onde a densidade da corrente do substrato é catódica. Uma estimativa de densidade de corrente local de deposição no entanto, indica que a velocidade de deposição sob a sonda é reduzida. Esses resultados são explicados pela presença de um campo elétrico entre a sonda e o substrato, o qual afeta a distribuição de potencial diretamente sob a sonda, produzindo um forte apantanhamento do fluxo difusional de íons Ag⁺.

The electrocrystallization process was studied in the system Ag(111)/Ag⁺, SO₄⁼ by *in situ* scanning tunneling microscopy (STM). The results show that Ag deposition occurs preferentially at step edges following a layer-by-layer growth mechanism, but polarization and imaging conditions greatly affect the local kinetics of this process. At STM-tip potentials more positive than the Ag/Ag⁺ equilibrium potential, a local dissolution of the substrate underneath the tip is observed even at low negative substrate overpotentials, at which the overall substrate current density is cathodic. An *in situ* STM imaging of Ag deposition was possible at sufficiently high negative substrate overpotentials. An estimation of the local deposition current density, however, indicates that the deposition rate underneath the STM-tip is reduced. These results are explained by the presence of an electric field between the STM-tip and the substrate, which affects the potential distribution directly underneath the tip, producing a large shielding of the diffusive flux of Ag⁺ ions.

Keywords: Scanning Tunneling Microscopy, STM-tip shielding effect, silver deposition, tip-induced dissolution

Introduction

The study of the mechanisms of electrochemical surface processes on metals, which involves structural changes of the electrode surface morphology, such as deposition and dissolution reactions or formation and dissolution of oxide layers, is theoretically and practically important. From the practical point of view, the electrodeposition process specially offers a controllable way of forming thin films and layered structures. Such interfacial electrochemical studies have been greatly

expanded over the past decade, because these processes can be directly monitored in real time using the Scanning Tunneling Microscopy (STM), which gives direct structural information at electrode surfaces and provides information concerning the progression of the electrochemical phenomenon and/or its reversibility.¹⁻⁴

However, for an *in situ* study of electrochemical phase formation processes, it is necessary to be aware of possible tip-substrate interactions and their effect on the interpretation of images acquired during the phase formation phenomena. The presence of the probing tip in the electrochemical cell produces a modification of the electrochemical environment due to the specific tip-substrate configuration. Recent studies related to the Cu electrodeposition on different substrates, showed that the

* e-mail: sgarcia@criba.edu.ar

Member of the Comisión de Investigaciones Científicas de la Pcia. de Buenos Aires, Argentina

STM-tip can significantly influence the local kinetics of electrochemical reactions by reducing mass transport of electrochemically active species, disturbing the electrochemical double layer and modifying the electric field.⁵⁻⁷ This influence was demonstrated not only by an inhibition of Cu electrodeposition but also by a local dissolution induced by the scanning STM-tip in the surface region beneath it. Winterlin *et al.*⁸ proposed that the tip-surface interactions are responsible for the enhancement in corrugation observed in STM images of the close-packed metal surfaces. Furthermore, Xiao *et al.*⁹ have suggested that this effect promoted by the STM tip can be used for local etching of metals, since the rate of local dissolution is better controlled than the usual use of electrochemical dissolution, as in the case for various types of tip-induced metal deposition for writing nanoscale structures. In addition, Guay *et al.*¹⁰ demonstrated that the tip-induced selective dissolution of aluminum may represent a convenient method for studying the stability and strength of passivating coatings. Thus, the structuring and modification of solid state surfaces in the nanometer or subnanometer range can be achieved using the STM-tip, which induces localized metal deposition or dissolution processes under appropriate polarization routines, constituting an important aim of modern science and nanotechnology. These previous results indicate that the possible influence of the STM-tip has to be taken into account in the analysis and interpretation of the STM experimental results.

In this paper we report *in situ* STM studies of the surface morphology changes due to the Ag deposition process on a Ag(111) single crystal in SO_4^{2-} containing acid solutions, under different polarization conditions, taking into account the influence of the STM-tip on the local deposition kinetics.

Experimental

A Ag(111) single crystal with a diameter of 0.65 cm was used as working electrode. Before each experiment the electrode surface was mechanically polished with diamond paste of decreasing grain size down to 0.25 μm and subsequently chemically etched according to a standard procedure¹¹ as described in a previous work.¹² After etching, the electrodes were thoroughly rinsed with fourfold quartz-distilled water.

The experiments were performed in $1 \times 10^{-4} \text{ mol L}^{-1} \text{ Ag}_2\text{SO}_4 + 1 \times 10^{-1} \text{ mol L}^{-1} \text{ H}_2\text{SO}_4$ solution, which was prepared from suprapure chemicals (Merck, Darmstadt) and fourfold quartz-distilled water. The solution was deaerated by nitrogen bubbling prior to each experiment.

In situ STM studies were carried out using a standard NanoScope III (Digital Instruments, Santa Barbara, CA, USA) and Pt-Ir tips isolated with Apiezon wax. Ag wires served as counter and reference electrode. The potentials of the STM tip (E_{tip}) and the Ag(111) substrate (E_{sub}) were independently controlled by a bipotentiostat.

Electrochemical measurements were carried out in a standard electrochemical cell with a three-electrode configuration under semi-infinite linear diffusion conditions, in order to characterize qualitatively the overall kinetics of delocalized Ag deposition and dissolution. A saturated mercury sulfate electrode and a platinum sheet (1 cm^2) served as reference and counter electrode, respectively. All electrochemical potentials are referred to the Nernst equilibrium potential $E_{\text{Ag}/\text{Ag}^+}$ of the 3D bulk Ag phase in the corresponding electrolyte solution.

Results and Discussion

The electrochemical behavior of the Ag(111) single crystal in the $1 \times 10^{-4} \text{ mol L}^{-1} \text{ Ag}_2\text{SO}_4 + 1 \times 10^{-1} \text{ mol L}^{-1} \text{ H}_2\text{SO}_4$ solution is illustrated in Figure 1 showing the corresponding steady state current-potential curve measured under semi-infinite linear diffusion conditions. The current density reaches at sufficient negative overpotentials ($\eta = E - E_{\text{Ag}/\text{Ag}^+} \ll 0$) a limiting value characteristic for a diffusion controlled deposition process. The electrochemical behavior of the deposition/dissolution processes is unsymmetrical and at high positive overpotentials ($\eta = E - E_{\text{Ag}/\text{Ag}^+} \gg 0$), the anodic current density increases due to the dissolution of the Ag(111) substrate. This process seems to have a relatively slow kinetic in relation to that observed in solutions containing other anions.¹² This inhibition is possibly related to the

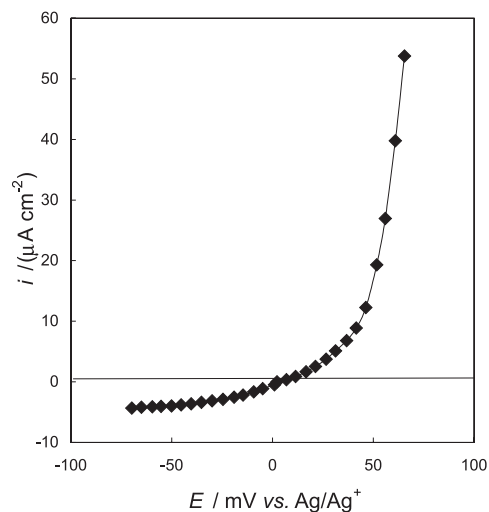


Figure 1. Steady state i - E dependence in the system Ag(111)/ $1 \times 10^{-4} \text{ mol L}^{-1} \text{ Ag}_2\text{SO}_4 + 1 \times 10^{-1} \text{ mol L}^{-1} \text{ H}_2\text{SO}_4$. $T = 298 \text{ K}$.

adsorption of SO_4^{2-} anions. It is well documented¹³⁻¹⁵ that sulfate or bisulfate anions could be specifically adsorbed on Ag(111) and they are also stronger adsorbed in comparison to other anions such as perchlorate.^{13,16,17} The sulfate adsorption on steps and kink sites present on the surface would result in a partial inhibition during the dissolution process.

Figure 2 shows an *in situ* STM image of the chemically polished silver surface, which typically consists of atomically flat terraces with mostly monatomic or diatomic steps. An average step density,¹ $L_s \cong 1.2 \times 10^6 \text{ cm}^{-1}$, was calculated taking into account an average terrace width of about 8 nm obtained by statistical analysis of a large number of STM images.

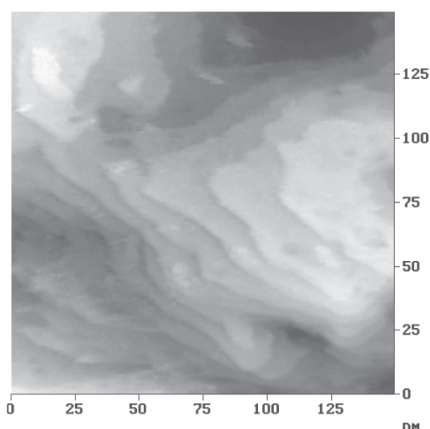


Figure 2. Typical *in situ* STM image of a polished Ag(111) surface.

At relatively low negative substrate overpotentials, $\eta_{\text{sub}} = -2.5 \text{ mV}$ and $E_{\text{tip}} = 26 \text{ mV}$, a local silver dissolution induced by the STM tip was observed (cf. Figure 3), although in this case the overall substrate current density was cathodic, namely, $i_{\text{sub}} = -0.9 \mu\text{A cm}^{-2}$. This local dissolution effect will be discussed later. The line scan STM image shown in Figure 3 is obtained by scanning the

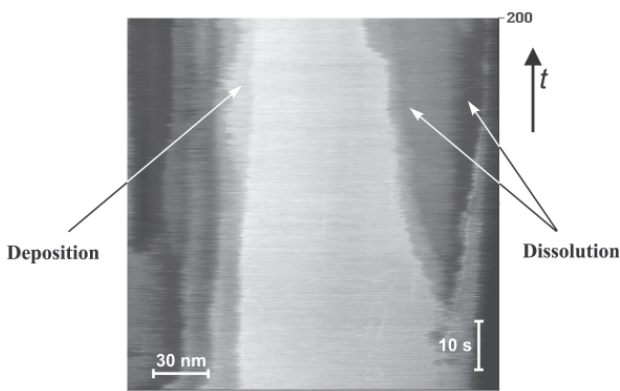


Figure 3. Line scan x-t STM image showing simultaneously dissolution and deposition zones. $\eta = -2.5 \text{ mV}$, $i = -0.9 \mu\text{A cm}^{-2}$, $E_{\text{tip}} = 26 \text{ mV}$, $I_{\text{tip}} = 10 \text{ nA}$. $T = 298 \text{ K}$.

Ag substrate surface repeatedly along a single line. This technique provides fast kinetic information about the deposition or dissolution at step edges because both phenomena can be rapidly recorded by this way. In Figure 3 both processes, deposition and dissolution could be seen simultaneously, together with non altered terraces. More clearly it is seen the local dissolution process, which occurs via a layer-by-layer dissolution mechanism. In a previous work,¹² it was demonstrated that also the dissolution process is locally affected by the STM-tip depending on the polarization conditions.

The tip-substrate interaction has been previously observed in the case of Pb electrodeposition on graphite,¹⁸ where the tip potential affected the Pb deposition in the area being imaged. In the present case, the tip induced selective dissolution was observed only applying positive tip potentials ($E_{\text{tip}} > E_{\text{Ag/Ag}^+}$) when the negative overpotentials were not relatively high. Generally, for a given electrolyte composition and a low negative substrate overpotential the local dissolution rate increases with increasing tip potential. In contrast, applying positive tip potentials, $E_{\text{tip}} = 10 \text{ mV}$, and relatively high negative substrate overpotentials, $\eta_{\text{sub}} = -60 \text{ mV}$, the silver deposition process underneath the STM-tip could be observed (Figure 4). This substrate potential is apparently negative enough to minimize the influence of the scanning STM-tip and to allow an imaging of Ag deposition. As it is shown in the series of STM images in Figure 4, a hole with frizzy edges originally present on the silver surface is gradually filled

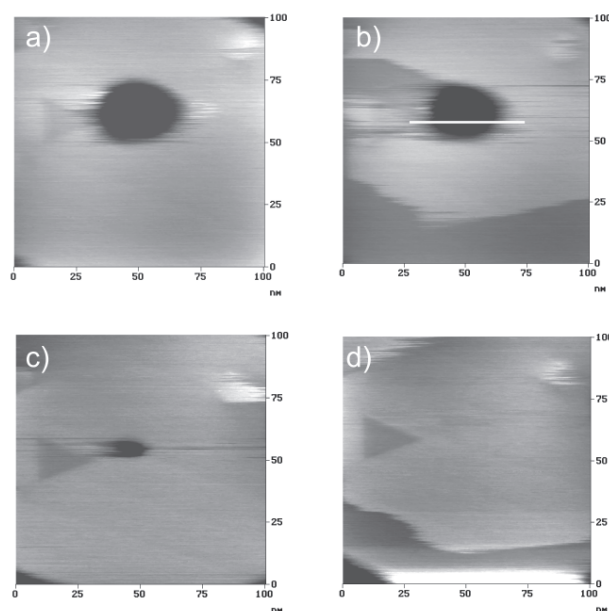


Figure 4. Sequential *in situ* STM images showing the deposition process at $\eta = -60 \text{ mV}$, $i = -4.1 \mu\text{A cm}^{-2}$. a) initial surface with a hole, and after b) 75 s, c) 403 s, d) 465 s. $E_{\text{tip}} = 10 \text{ mV}$, $I_{\text{tip}} = 8 \text{ nA}$. $T = 298 \text{ K}$.

up as Ag deposition proceeds, forming a large terrace at $t = 465$ s. The gradual filling of the hole is displayed in Figure 5a where the tip was scanned repeatedly along a single line crossing the hole in the location indicated in Figure 4b. The corresponding cross sections are shown in Figure 5b. A propagation rate of step edges of about $v_{\text{dep}} \cong 4 \times 10^{-9}$ cm s⁻¹ could be determined from the line scan STM images in Figure 5. This value can be used for an estimation of the corresponding local deposition current density from the equation:¹

$$i_{\text{dep}}^{\text{local}} = -q_{\text{mon}} v_{\text{dep}} L_S \quad (1)$$

where q_{mon} is the charge density of a Ag(111) monolayer and L_S is the average step density. Considering $q_{\text{mon}} = 220$ $\mu\text{C cm}^{-2}$, $L_S = 1.2 \times 10^6$ cm⁻¹, and $v_{\text{dep}} \cong 4 \times 10^{-9}$ cm s⁻¹, a local deposition current density of $i_{\text{dep}}^{\text{local}} = -1.1$ $\mu\text{A cm}^{-2}$ is estimated. This value is about four times lower than the overall cathodic substrate current density $i_{\text{sub}} = -4.1$ $\mu\text{A cm}^{-2}$ measured in the system at $\eta_{\text{sub}} = -60$ mV and indicates that an influence of the STM-tip on the deposition process is still present.

The above results show that electrocrystallization of Ag on Ag(111) follows a layer-by-layer growth mechanism. This behavior is in agreement with the silver deposition on Au(100) and Au(111) substrates after the deposition of the first silver monolayers.^{2,19} In that case, the formation of the underpotential Ag layer that depends on the substrate orientation, is the precursor to the overpotential deposition, *i.e.*, the Ag UPD monolayer is involved in the

initial steps of the nucleation and growth processes in the overpotential range. Once the silver monolayer on Au(hkl) is formed, and due to a negligible adsorbate/substrate misfit, the subsequent deposition process occurs as on the same substrate, following a layer-by-layer growth mode.

In situ STM imaging of Ag electrocrystallization on Ag(111) shows often an appearance on growing surface terraces of shallow triangular pits, characterized by a flat bottom and a depth of about 1/3 of the monolayer. An example of the appearance of such a triangular pit is seen in Figures 4c,d. The appearance of these pits is attributed to stacking faults which intersect the Ag(111) surface forming “imperfect” steps with a height of 1/3 of the height of a perfect monatomic step.^{1,20,21} Figure 6a shows a zoom of Figure 4d with both a perfect and an “imperfect” step (cf. Figure 6b). Due to the high dynamics of kink atoms the perfect step appears frizzy in the STM image. In contrast, the “imperfect” step does not contain kink sites and is not active during the deposition process. The surface of the large Ag terrace formed, revealed the hexagonal atomic corrugation of the Ag(111) with the 0.29 ± 0.01 nm interatomic spacing (Figure 6c). The absence of atomic structures that could be associated with anion adsorption on Ag(111) may be a consequence of a relatively delocalized adsorbed anions or the STM-tip interaction sweeping them away from the surface imaged.

The inhibition of the cathodic deposition of silver and the local dissolution observed in the present study can be explained considering the influence of the STM tip on these processes. The tunneling tip in the electrochemical system can be considered as a new electrode that in general will change the electrostatic fields in the neighboring electrolyte. Specially, if the tunneling tip comes close to the sample surface it will modify the electrochemical potential there. The tip proximity impedes, to some extent, the diffusion of ions through the neighboring electrolyte, and depending on the tip potential, it will induce faradic growth or dissolution processes. In the present conditions, the existence of an electric field between tip and substrate can affect the potential distribution, making the area directly below the tip less negative than the rest of the surface and insufficient for the deposition of Ag. Consequently, there will be a very large shielding of the diffusive flux of Ag⁺ ions to the areas under study, which only a rather thin layer of electrolyte exists between the tip and the underlying surface. Therefore, the decrease in the growth rate of Ag should be attributed to the decrease in the local concentration in the region where the tip was scanned. A possible explanation of the tip-induced electrochemical etching observed in the previous results is based upon electrostatic considerations and involves

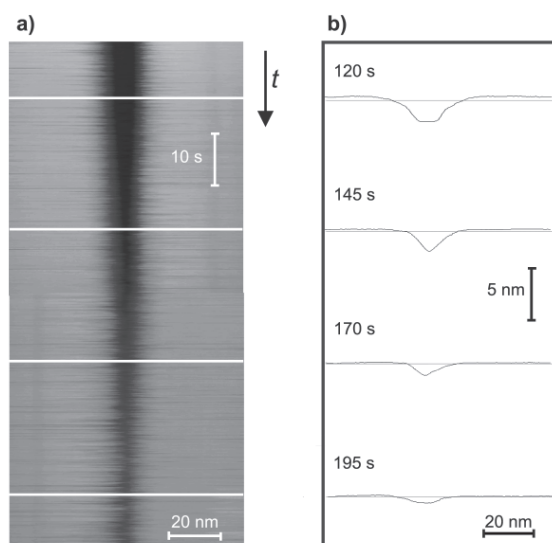


Figure 5. a) Line scan x-t STM image obtained by scanning along the horizontal line indicated in the hole region of Figure 4b; and b) the corresponding cross sections along the lines indicated in a). Image conditions: $\eta = -60$ mV, $i = -4.1$ $\mu\text{A cm}^{-2}$, $E_{\text{tip}} = 10$ mV, $I_{\text{tip}} = 8$ nA. $T = 298$ K.

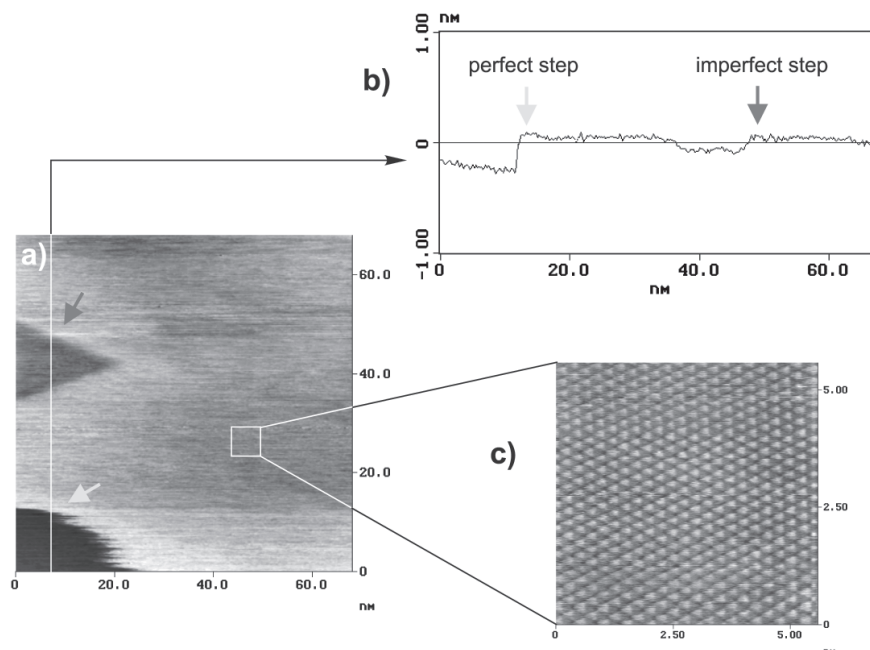


Figure 6. *In situ* STM image of the Ag(111) surface with: a) perfect and imperfect steps; b) cross section showing imperfect steps with a height of 1/3 monolayer; c) atomic resolution obtained on an atomically flat Ag(111) terrace. Image conditions: $\eta = -60$ mV, $i = -4.1 \mu\text{A cm}^{-2}$, $E_{\text{tip}} = 10$ mV, $I_{\text{tip}} = 8$ nA. $T = 298$ K.

the electrostatic repulsion of Ag^+ ions by the positively charged tip. This would lower the Ag^+ ion concentration in the vicinity of the tip and, hence, shift the local Nernst equilibrium potential for the Ag surface underneath the tip to more negative values. By this way, a localized dissolution, or a reduction on the local silver deposition rate is induced, in relation to the global deposition process of the surface.

Recently, Chi *et al.*²² have discussed the mechanism of pit formation induced by the STM-tip on Au(111) surface in aqueous environment. In that case the nanopits were implemented scanning in a reduced area but with a extremely small bias potential and in potential region of the substrate where no faradic process is involved. They proposed a mechanism of pit formation based on local surface reconstruction induced by electronic contact between tip and substrate. In contrast, the results shown in the present paper seem to be more related with a change in the local equilibrium potential underneath the tip and in agreement with the results obtained recently by Xie and Kolb⁶ with the system Cu/Cu²⁺.

Conclusions

The results show that in SO_4^{2-} containing electrolytes the local kinetics of the electrochemical deposition of silver on Ag(111) during the *in situ* STM surface imaging depend strongly on the polarization and tunneling

conditions. A local dissolution of the Ag(111) substrate is observed even at low negative overpotentials, at which the overall substrate current density is cathodic. This local dissolution is attributed to a shielding effect induced by the STM-tip. This phenomenon is based on a change in the silver concentration underneath the STM-tip, promoted by an electrostatic repulsion of Ag^+ ions by the positively charged tip and by mass transport limitations. The silver deposition underneath the STM-tip could be observed at relatively high negative substrate overpotentials where the interference due to the scanning tip was not so pronounced. The Ag electrocrystallization process follows a layer-by-layer mechanism.

However, a better understanding of the mechanism of these phenomena requires further experiments such as a systematic variation of tip and substrate potentials in order to clarify the complex tip-substrate interactions. These studies are in progress.

Acknowledgements

The authors gratefully acknowledge the financial support of this work by the Universidad Nacional del Sur, Bahía Blanca (Argentina), DFG (Deutsche Forschungsgemeinschaft), DAAD (Deutscher Akademischer Austauschdienst), BMWi (Bundesministerium für Wirtschaft) and AiF (Arbeitsgemeinschaft industrieller Forschungsvereinigungen).

References

1. Budevski, E.; Staikov, G.; Lorenz, W. J.; *Electrochemical Phase Formation and Growth – An Introduction to the Initial Stages of Metal Deposition*, VCH: Weinheim, 1996.
2. García, S. G.; Salinas, D. R.; Mayer, C. E.; Pauling, H.-J.; Vinzelberg, S.; Staikov, G.; Lorenz, W. J.; *Surf. Sci.* **1994**, *316*, 143.
3. García, S. G.; Salinas, D. R.; Mayer, C. E.; Schmidt, E.; Staikov, G.; Lorenz, W. J.; *Electrochim. Acta* **1998**, *43*, 3007.
4. Kolb, D. M.; *Electrochim. Acta* **2000**, *45*, 2387.
5. Stimming, U.; Vogel, R.; Kolb, D. M.; Will, T.; *J. Power Sources* **1993**, *43-44*, 169.
6. Divisek, J.; Steffen, B.; Stimming, U.; Schmickler, W.; *J. Electroanal. Chem.* **1997**, *440*, 169.
7. Xie, Z.-X.; Kolb, D. M.; *J. Electroanal. Chem.* **2000**, *481*, 177.
8. Winterlin, J.; Wiechers, J.; Brune, H.; Gritsch, T.; Höfer, H.; Behm, R. J.; *Phys. Rev. Lett.* **1989**, *62*, 59.
9. Xiao, X.; Berenz, P.; Baltruschat, H.; Sun, S.; *J. Electroanal. Chem.* **2001**, *500*, 446.
10. Rouè, L.; Chen, L.; Guay, D.; *Langmuir* **1996**, *12*, 5818.
11. Höpfner, M.; Obretenov, W.; Jüttner, K.; Lorenz, W. J.; Staikov, G.; Bostanov, V.; Budevski, E.; *Surf. Sci.* **1991**, *248*, 225.
12. García, S. G.; Salinas, D. R.; Mayer, C. E.; Lorenz, W. J.; Staikov, G.; *Electrochim. Acta* **2003**, *48*, 1279.
13. Smolinski, S.; Zelenay, P.; Sobkowski, J.; *J. Electroanal. Chem.* **1998**, *442*, 41.
14. Stevenson, K. J.; Gao, X.; Hatchett, D. W.; White, H. S.; *J. Electroanal. Chem.* **1998**, *447*, 43.
15. Marinkovic, N. S.; Marinkovic, J. S.; Adzic, R. R.; *J. Electroanal. Chem.* **1999**, *467*, 291.
16. Vitanov, T.; Popov, A.; Sevastyanov, E. S.; *J. Electroanal. Chem.* **1982**, *142*, 290.
17. Sneddon, D. D.; Sabel, D. M.; Gewirth, A. A.; *J. Electrochem. Soc.* **1995**, *142*, 3027.
18. Hendrick, S. A.; Kim, Y-T; Bard, A. J. ; *J. Electrochem. Soc.* **1992**, *139*, 2818.
19. García, S. G.; *PhD. Thesis*, Universidad Nacional del Sur, Bahía Blanca, Argentina, 1997.
20. Wolf, J. F.; Ibach, H.; *Appl. Phys. A* **1991**, *52*, 218.
21. Guiesen, M.; Dietterle, M.; Stapel, D.; Ibach, H.; Kolb, D. M.; *Surf. Sci.* **1997**, *384*, 168.
22. Chi, Q.; Zhang, J.; Friis, E. P.; Andersen, J. E. T.; Ulstrup, J.; *Surf. Sci.* **2000**, *463*, L641.

Received: November 10, 2003

Published on the web: November 18, 2004